EPFL

Functional mapping of remote fear memory extinction

Author:
Célia Benquet

Supervisor:
Dr. Bianca Silva

Contents

Abstract

Traumatic events can lead to the formation of some of the most tenacious long-term memories, which may favor post-traumatic stress disorder. Nowadays, one of the most efficient solutions consists in an extinction training. The patient is repeatedly exposed to the trauma-inducing stimulus in a safe environment to attenuate the fearful component of the trauma-related memories. If several previous reports have discussed the neuroanatomical correlates in recent (eg. 1-day-old) fear memories extinction, only few is known about remote (eg. 30-day-old) fear memory extinction. A recent unpublished investigation from Silva et al. shows that the extinction of remote fear memory depends on thalamic nucleus reuniens (NRe) outputs to the basolateral amygdala (BLA). To validate this experiment and in order to formulate a better activation map at both recent and remote fear memory extinction, other regions implicated in memory storage were investigated for these two types of memory extinction. Using a combination of activity-dependent neuronal circuit mapping network connectivity analysis, this report investigates the role of the hippocampus in recent fear memory extinction. The results suggest that hippocampal projections - including especially the CA1 and Sub - to the NRe or the BLA do not play a role in fear extinction for recent fear memory.

1 Introduction

When experiencing fear or strong trauma, one can develop some of the most persistent forms of memory, which contributes to the prevalence of stress and anxiety-related disorders. One of the most effective treatments for patients suffering from such post-traumatic stress disorders (PTSD) is exposure therapy. This behavioral psychotherapy consists in attenuating traumatic memories by repeated exposure of trauma-inducing stimuli in a safe environment [1][2]. Consequently, a weakening of the aberrant emotional responses associated with the fear-related memory can be observed [3]. If the underlying brain circuitry remains largely unknown, most importantly it has been shown that the intervention loses efficiency the further it is delayed from the original trauma [4]. In view of this, early interventions are considered as an essential part of the treatment. Yet, such interventions are not always available for the patient as traumata often originate from a distant past event. Hence, identifying treatments options for remote traumata remains of utter value.

Using fear extinction as an experimental model of exposure therapy, previous studies have widely investigated and identified brain circuits implicated in fear memory attenuation [5]. However, most of those studies focused on the neural substrates of recent (eg. 1-day-old) fear memory attenuation and less is known about the neural circuitry mediating remote (eg. 1-month-old) fear memory attenuation. Investigation of this gap of knowledge appeared as a crucial need. Indeed, with time, traumatic memories are consolidated through a re-organization of the circuitry of memory storage [6]. It implies that the extinction of remote memories may rely on different brain networks than the ones implicated in recent memory storage.

In light of those observations, Silva et al. established a systematic comprehensive map of brain activation upon remote fear memory attenuation in mice [7]. Mice were first subject to an efficient extinction training paradigm for 1-month-old contextual fear memory attenuation. Then, immunohistochemistry (IHC) and network connectivity analysis were combined on different regions of the brain that are known to be implicated in recent and remote memory storage. This led to the identification of relevant brain areas as potential targets for therapeutic approaches against distant traumatic memories, requiring a deeper investigation.
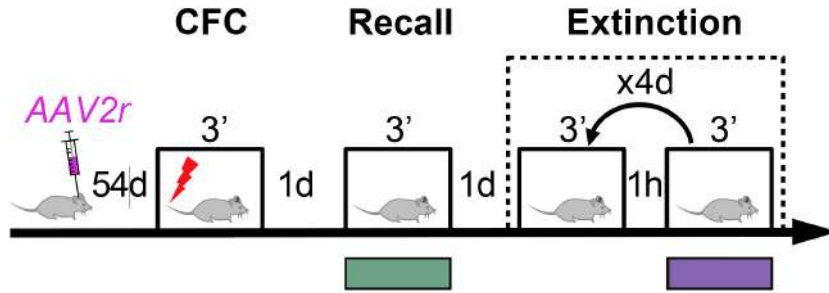
2

Figure 1: Schematic representation of the behavioral paradigm for recent fear memory extinction. 54 days after viral tracer injection mice underwent contextual fear conditioning (CFC). One day after, animals were re-exposed to the conditioned context in the absence of foot shock (Recall) and, subsequently, to the spaced remote fear memory extinction paradigm consisting of two sessions of context exposure per day for four days (Extinction). Control animals did not receive foot shocks during fear conditioning, but underwent the extinction procedure (No shock).

The study notably reported that there seems to be no correlation between the ventro-medial prefrontal cortex (mPFC), particularly the infralimbic cortex (IL) and basolateral amygdala (BLA) at remote extinction. However, previous studies showed that the interplay between the IL and the BLA plays an essential role in the fear attenuation induced by recent exposure therapy-extinction protocol taking place 1-2 days after conditionning [8]. Consequently, and as it has never been investigated in relation to remote fear memory extinction, Silva et al. continued their study on neural correlates of remote fear memory extinction, focusing on the implication of the IL-BLA pathway.

Recent unpublished findings show that if the IL projections to BLA are not extensively activated at remote fear memory extinction, IL to thalamic nucleus reuniens (NRe) and NRe to BLA projections are. Moreover, alternative pathways from other brain areas implicated in remote memory storage to the BLA and NRe were extensively studied, as it was never really investigated before. It includes parts from the cortex, midbrain, midline thalamus and hippocampus, the latest being of particular relevance for the project. Results at remote extinction showed no significant activity for those projections with the exception of the ventral tegmental area (VTA) in the midbrain and the IL.

In order to validate those findings as well as investigate the neuronal connectivity at recent extinction, the experiment was reproduced using the same experiment setup but with a recent fear memory extinction paradigm, presented on Figure 1. Focusing on the implication of the hippocampus in the recent fear extinction process, previous studies presented its importance at recent extinction recall [9] and its role as a regulator of the context-specificity in fear extinction [10]. It was also found that the hippocampal-mPFC pathway is associated with the extinction processes of context-dependant fear memory [11]. This project consists in studying more precisely the role of the hippocampal-NRe and hippocampal-BLA pathways in recent fear memory extinction, that was never really investigated.

2   Methods

The present semester project includes a full range of methods starting from freezing of freshly acquired mice brains to the acquisition of the final results. The step-by-step process is summarized on Figure 2 and the image analysis is more particularly detailed.

Mice were initially exposed to an efficient recent fear memory extinction paradigm pre-

Figure 2: Step-by-step process of the methods used in the project.

sented on Figure 1. As we aimed at studying neuronal connectivity and neuronal activation at extinction, we combined cFos-based neuronal activity mapping and retrograde tracing. For retrograde tracing, the brains were injected with AAV2r-*Tomato* and AAV2r-*GFP* retrograded tracers in respectively the BLA and NRe regions. Those viruses infect synaptic terminals and are retrogradely transported to the pre-synaptic somata [12]. We focused on the presynaptic neurons located in the hippocampus. As for cFos expression, mice were sacrificed 90 min after behavioral testing in order to analyze neuronal activity at the last extinction session using cFos IHC. Brains were then removed and post-fixed (4% PFA overnight).

2.1   Brain freezing and cutting

The wet part of the project took place on mice brains from the experimental group WT48, composed of 12 animals. The post-fixed brains were retrieved to get cryoprotected (30% sucrose, 1X PBS, 4°C, 48h) and frozen at -80°C.

Then, 40 μm coronal sections were cut using a sliding microtome (Thermo Scientific, Microm HM 450). By removing the anterior part of the brain (olfactory bulbs), all slides were collected until the cerebellum was reached. The cut slices were then immediately stored in antifreeze at -80°C.

2.2   cFos immunohistochemistry protocol

From the obtained slides, 2 slides for the ventral hippocampus and 3 slides for the other studied areas (except prefrontal cortex) were selected per brain. The rest of the slides were bottled in antifreeze and stored at -80°C for back-up use. Then, a cFos IHC protocol was performed on the selected slides. Free floating sections were incubated in blocking solution (1% BSA, 1X PBS, 0.3% TritonX100, Sigma) at room temperature for 1 h, followed by incubation with rabbit anti-cFos antibody (1:5000, Synaptic System, #226 003) in blocking buffer (1% BSA, 1X PBS, 0.1% TritonX100) overnight at 4°C under constant shaking. Sections were washed extensively with PBS Triton 0.1% and then exposed to secondary antibody (Alexa Fluor 647-conjugated donkey anti-rabbit IgG, Life Technologies) in blocking buffer at room temperature for 2 h. They were incubated with Hoechst (Life Technologies) at 1:1000 in PBS at room temperature for 5 min, washed extensively with PBS and mounted on superfrost glass slides (ThermoScientific) with Fluoromount mounting medium (SouthernBiotech).

Images were acquired on a virtual slide microscope (VS120, Olympus) with a 10X objective.

2.3   QuPath image analysis

Both images from WT48 and WT47 sections were analyzed using QuPath v0.1.4-SNAPSHOT [13] for cFos, AAV2r-Tomato, AAV2r-GFP and Hoechst positive cell detection.

For each glass slide, microscopy acquired data are composed of an image of the side label (Fig. 3a), an overview of the glass slide (Fig. 3b) and individual images of each mounted section similar to the one presented on Figure 3d. Those data are regrouped in a folder and
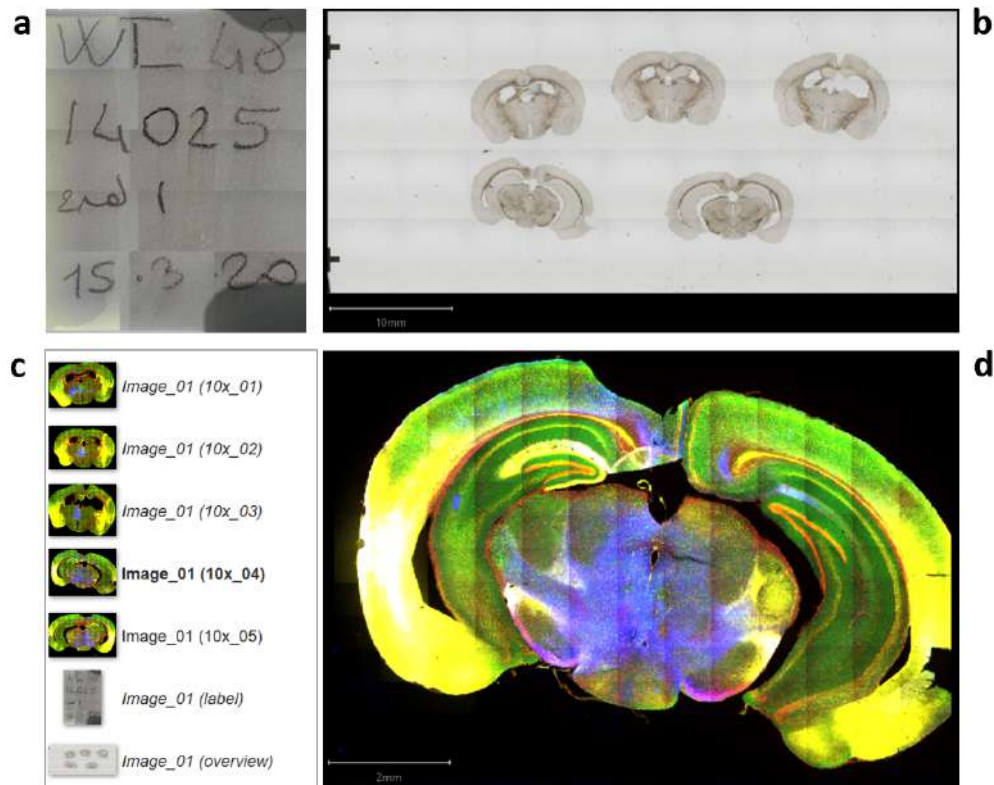
Figure 3: Example of the set of images obtained for one brain (here, Mouse 14025, WT48), regrouped in a single VSI file (here, *Image_01.vsi*). **a.** Annotated label on the glass slide. **b.** Overview of the glass slide. We can see 5 different sections. **c.** Left panel on QuPath, review of the different images available. **d.** Example of individual image for one section (here, Image_01 (10x_04)). One for each section is obtained.

can be accessed through the corresponding .vsi file on QuPath. For example, *Image_01* for WT48 contains all the data corresponding to Mouse 14025 (see Fig. 3). Then, on QuPath, sub-images are found and the first image would be called *Image_01 (10×_01)* (Fig. 3c).

2.3.1 Regions outlining and classification

The process to treat brain sections images from an opened QuPath application is detailed below and commands of interest are shown on Figure 4. Regions that presented irregularities such as a fold or regions that were too caudal were not outlined and are not taken into account for the rest of the analysis. A detailed list of those irregularities is presented in the ReadMe file.

- From the initial interface of the application, by clicking on `Create project`, the folder in which the VSI files are stored is selected.

- Then, those VSI files need to be added to the project by going to `Add images`, followed by `Choose files` to select them.

- By clicking on an image on the left panel (in the *'Project'* tab), it appears on the right. We were interested in analyzing the two last sub-images for each *Image* (the 2 sections representing the ventral hippocampus for an individual brain).

- Once a section is selected, areas of interest can manually be outlined by using the `Polygon tool`. Based on the Hoechst signal (red on QuPath) and following the Allen Brain Reference Atlas [14], the dendate gyrus (DG), hippocampus subfields CA1 and CA3 and the subiculum (Sub) on both hemispheres are outlined.
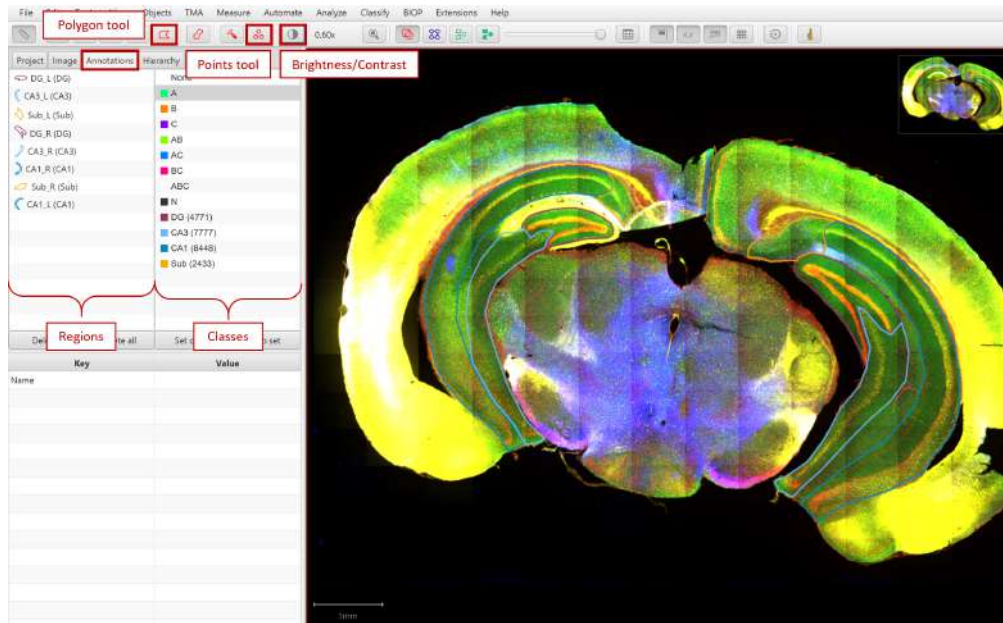
5

Figure 4: QuPath interface. Positions of the different buttons of use are highlighted in red.

- By going to `Annotations` in the left panel, right clicking on the region and selecting `Set properties`, outlined regions can be renamed. The regions need to be renamed by a combination of their scientific abbreviation and a distinctive sign of its lateral position (either in the left (L) and right (R) hemisphere). A way of naming can be seen on the regions panel on Figure 4.

- The regions also need to be classified. Similar regions from one hemisphere to the other are grouped together. A class is created by right clicking in the class panel (see Fig. 4) and selecting `Add class`. A way of naming classes is shown in the classes panel on Figure 4. it should correspond to the abbreviation of the area.

2.3.2 Tuning the threshold

For co-localization analysis of AAV2r-Tomato (projection to BLA), AAV2r-GFP (projection to NRe), cFos and Hoechst positive cells, a custom-built script for QuPath was used. Positive neurons within the outlined structures can automatically be detected by running a GROOVY file script directly on QuPath. To do so, one needs to manually tune the intensity threshold at which they are detected in a trial-and-error way on the script until the detection takes into account most of them.

The main file, *qps-multiChannels_PositiveCells_Analysis.groovy*, is able to detect co-localization of the tracer and the markers in the neurons by running on different channels at once, but takes a certain time to compute. Hence, we preferably tuned the threshold, channel by channel, on the lighter *cell_detection_cFos.groovy* file while the final results were obtained from the main one. Table 1 summarizes the possible classes to which a neuron can be attributed to when detection is performed with the main script.

As finding the perfect threshold for each region and each channel (markers and tracers) would take a certain amount of time even on the lighter script and considering that a manual counting takes place afterward, choices were made to simplify the process and are stated bellow.

- The higher the threshold, the lower the number of detected cells. In other words, if the threshold is high, only regions with a very high intensity are detected.

6

Table 1: Summary of possible detections. Output detection for a given cell can be N, A, B, C, AB or AC. Hoechst marker (Channel 1 on QuPath) fixates to all cell nuclei and permits to detect individual neurons, regardless of their activity or projection. Hence all detected cells are at least detected as N. Then, cFos marker (Channel 2) fixates to the nucleus of cells that got activated at extinction. It means that A-detected cells were active at extinction. Finally, for the tracers, analyzed separately, if the cell projects to the NRe, respectively BLA, it is detected as B (Channel 3), respectively C (Channel 4) and if it also was active at extinction then it is labelled as AB, respectively AC. The table presents all possible detections, the situation in which it can appear (which tracer is analyzed) and the significance regarding the cell activation and connectivity.

Output detection	Possible apparition	Significance for the cell
N	Both tracers	Non-implicated
A	Both tracers	Activated at extinction
B	For tracer B	Projections to the NRe
C	For tracer C	Projection to the BLA
AB	For tracer B	Presents characteristics of A and B
AC	For tracer C	Presents characteristics of A and C

- Threshold for Hoechst positive cells (Channel 1) was taken as the same for all images of the experiment.

- Except in particular cases where the difference is too important, all outlined structures were regrouped to find a common threshold for each channel of a section.

- The threshold was taken at the higher end of the range of possibilities. That means that if, for example, the perfect threshold for a given channel for the DG class (DGs in both hemispheres) is at 120 but only at 60 for the CA3 regions, we still keep 120 as the threshold for all classes in the section for this channel. This choice facilitates the manual cell detection assessment (later, in Section 2.3.4), as it is easier to add cells than to remove them from the automatically-performed count.

- Threshold values were regrouped in a .csv file to be used later for the main script. We call it the *Parameters* file. Even if it is the same for all regions, we still detailed the different regions to be able to note anomalies or bugs during the different computational tasks.

The threshold was tuned through the following steps.

- *cell_detection_cFos.groovy* was opened on QuPath by sliding the file to the application. No line needs to be changed, except lines 30 and 35.

- The channel number was precised after `detectionImageFluorescence`. It corresponds to the tracer/marker the script needs to detect. The values are 1 to detect Hoechst positive cells (all neurons), 2 for cFos positive cells (neurons activated at extinction), 3 for AAV2r-GFP positive cells (projection to the NRe) and 4 for AAV2r-Tomato positive cells (projection to the BLA).

- The threshold value is modulated at `threshold`.

- The `Brightness/Contrast` button allows to only keep the channel of interest by deselecting the others.

- By pressing the `H` key, one can remove the detection shapes from the image to easily check that there is indeed a cell to detect or not.

2.3.3 Main detection script

Once all the threshold values were determined and stored in the .csv file, the heavier script *qps-multiChannels_PositiveCells_Analysis.groovy* was run.

- First, the outlined regions need to be attributed to a class (see Section 2.3.1) and the script opened in QuPath.

- From line 104 to 106, the channels indexes were specified. ChA corresponds to channel 2 (cFos+), chB to 3 (AAV2r-GFP+) and chC to 4 (AAV2r-Tomato+). As the script takes a long time to run, it can only be run for one of the two tracers. The corresponding channel was set to the corresponding number while the other one needed to be set to `null`.

- Line 108, `def annotationName` corresponds to the class (ensemble of the 2 similar outlined regions) to run the script on.

- Then, there are 4 similar *DetectorParams.builder()*, one for each of the channels. The `.threshold` line was set for each to correspond to the values found in the previous step and stored in the *Parameters* file.

- The script was run for each class and for both tracers. We kept track of the process using the *Parameters* file by highlighting the run classes.

- The output of the script on one class for one tracer is composed of the detection shapes on the image and an output .csv file that contains especially the count of Hoechst+, cFos+, AAV2r+ (-Tomato or -GFP) and double positive (cFos+ and AAV2r+) cells.

- If regions are analyzed for one tracer and then for the second, the results of the second are erased, same thing for the output .csv file. Hence, the output results can either be duplicated to run the script for the second tracer on the duplicated image or entirely analyzed (manual check) before running the script for the second tracer. We decided to perform the manual checking for one tracer before running the script for the second tracer.

2.3.4 Manual counting

Once all classes have been run for a section, the output .csv file gives a detailed count of the detected cells. This file needs to be checked and eventually modified by manually recounting the cells on the image. To do so, the `Points tool` is of great use. Once the file has been assessed,

- the column name for the area was changed to `Area um^2`. This comment applies for French Excel that uses the unit μm instead of *um*.

- the file was renamed with the number of the corresponding mouse and the number of the section. For example, file *Image_01 (10×_04)* becomes *14025_04*.

- the file was placed into a folder corresponding to the studied tracer (either B or C).

2.4 Python script and visualization of the results

Once all the output files for a tracer were obtained and their values manually assessed, a Python script was used to compute the final results.

The final output is constituted of a main .csv file with the results over all the animals of an experimental group as well as a .csv file for each animal containing raw numbers for each region of each section. Those raw files are regrouped in a folder. The resulting main .csv file presents a certain number of ratio on the different detections used to calculate a chance ratio. If less than 4 cells were detected for a given category, the region was discarded. Chance ratios were calculated for each outlined region with the following formula and averaged across the 2 sections for each animal:

$$Chance\_Ratio = \frac{[Double+]}{[Hoechst+]} \times \frac{[Hoechst+]^2}{[cFos+][AAV2r+]} \tag{1}$$

The script is constituted of 2 files. The one which is modifiable by the user is *CSV_reader.py*. It needed to be adapted to the experiment by setting the parameters in the part *Parameters that you have to set*. Below, we list the different parameters to adapt.

1. `param_list`: list of the information to get from the output .csv files. For a tracer, it corresponds to the name of the area it was injected in. For our experiment, for NRe projections analysis: *['DAPI','cFos','NRe','area','NRe_cFos']*.

2. `tracer`: corresponding analyzed tracer, by the name of the area it was injected in. For our experiment, for NRe projections analysis: *'NRe'*.

3. `region_list`: list of the different areas that appear in the .csv file (name of the classes). For our experiment: *['DG', 'CA3', 'CA1', 'Sub']*.

4. `combine`: if a whole region can be separated into sub-regions. Keys of the dictionary are whole regions and values are lists of sub-regions. For our experiment, each region is already a whole region so we had to rewrite it as its only sub-regions.

5. `origin` and `root`: path to the main folder and the Excel files folder.

6. `recall`, `extinction` and `control`: lists of the mice numbers associated to their experimental group. For our experiment, we only fill the *'extinction'* and *'control'* lists.

7. `title`, `output_file` and `raw_number_directory`: title of the results, name of the output file and path to the folder containing raw numbers results respectively. For our experiment, for NRe projection analysis: *'WT48 retro recent hippocampus → NRe'*, *root + '/Results_NRe_WT48.csv'* and *root + '/Raw_numbers_NRe_WT48'*.

2.5 Statistical analysis

Data analysis was performed with PRISM 8 software (GraphPad). All data are reported as mean ± standard error. The target number of animals used in each experiment was determined based on numbers in previously published studies.

3 Results

Final results are presented on Figures 5a and 5b. They regroup results for both WT48 and WT47 and depict the chance ratio of having cells in CA1 (and in Sub for projections to NRe) that are activated at extinction and that project to, respectively, the NRe (Fig. 5a) and the BLA (Fig. 5b) areas for both experiment groups (control animals and animals who underwent an extinction paradigm).
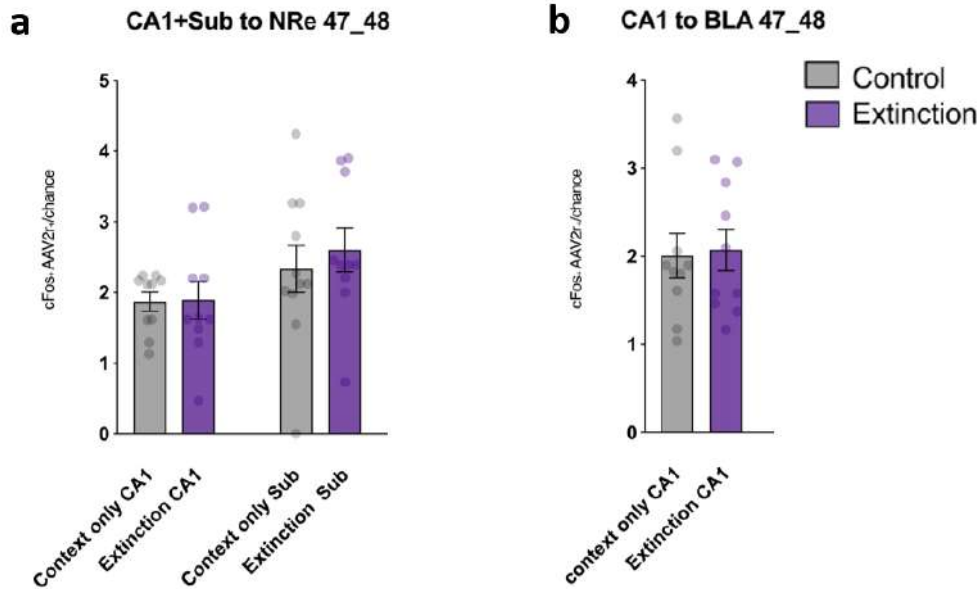

Figure 5: Colocalization analysis of retrogradely traced cells from respectively **a.** the NRe (AAV2r-GFP+)and **b.** the BLA (AAV2r-Tomato+) and cells activated upon remote fear memory extinction (cFos+) in hippocampus for WT48 and WT47. Analysis is done on 12 (WT48) + 8 (WT47) = 20 mice with 10 individuals in each group. Regions were discarded if less than 4 neurons were detected for a given tracer.

4 Discussion

We see no significant difference between the control chance ratio and the extinction chance ratio on both graphs. Hence, the neurons that project to either the NRe (Fig. 5a) or BLA (Fig. 5b) in the hippocampus are not significantly active at recent fear extinction. The hippocampal-NRe and hippocampal-BLA pathways do not seem to be implicated in fear extinction.

Even if the results are non-significant, potential sources of errors need to be taken into account. Detection on QuPath is partly human-curated considering that both the threshold and the manual assessment of the detection is based on observations only. Moreover, we selected 2 sections for each mouse, meaning 4 times the same regions for one animal. In some cases, sections were too caudal or badly mounted and its entirety or part of it had to be dismissed from the analysis. We also discarded regions in which less than 4 cells were detected for a given tracer. In that respect, results could be somewhat unbalanced between control and extinction groups and average on a single animal could rely on only one region (if the 3 others are discarded). Finally, the individual points on the graphs are distributed over a wide range of values. Even if the standard error bar is of reasonable width, maybe a higher number of animals in each group could favor a closer range of values and a better statistical analysis.

As other studies showed that the hippocampus is implicated in recent extinction recall, further investigations on the role of the two studied pathways in extinction recall could be of interest. Moreover, results from a previous paper from Silva et al. showed a high correlation in activity as well as a high network connectivity between the NRe and the hippocampus, especially the ventral DG and CA1 at remote fear extinction recall [7]. A similar investigation as the current one but this time focusing on fear extinction recall with both remote and recent extinction paradigms could provide insights on the neuronal mechanisms in the organization of fear-related memories.

References

[1] Edna B. Foa and Michael J. Kozak. Emotional processing of fear: Exposure to corrective information. - PsycNET, 1986. [Online; accessed 17. Jun. 2020].

[2] E. B. Foa. Psychosocial Treatment of Posttraumatic Stress Disorder. *J. Clin. Psychiatry*, 61(Suppl):5, 2000.

[3] Judith Cukor, Megan Olden, Francis Lee, and JoAnn Difede. Evidence-based treatments for PTSD, new directions, and special challenges. *Ann. N.Y. Acad. Sci.*, 1208(1):82–89, Oct 2010.

[4] Xianli An, Ping Yang, Siguang Chen, Fenfen Zhang, and Duonan Yu. An Additional Prior Retrieval Alters the Effects of a Retrieval-Extinction Procedure on Recent and Remote Fear Memory. *Front. Behav. Neurosci.*, 11, Jan 2018.

[5] Cyril Herry, Francesco Ferraguti, Nicolas Singewald, Johannes J. Letzkus, Ingrid Ehrlich, Andreas Lüthi, Cyril Herry, Francesco Ferraguti, Nicolas Singewald, Johannes J. Letzkus, Ingrid Ehrlich, and Andreas Lüthi. Neuronal Circuits of Fear Extinction. *Eur. J. Neurosci.*, 31(4):599–612, Feb 2010.

[6] Paul W. Frankland and Bruno Bontempi. The organization of recent and remote memories. *Nat. Rev. Neurosci.*, 6(2):119–130, Feb 2005.

[7] Bianca A. Silva, Allison M. Burns, and Johannes Gräff. A cFos activation map of remote fear memory attenuation. *Psychopharmacology*, 236(1):369–381, Jan 2019.

[8] Daniel W. Bloodgood, Jonathan A. Sugam, Andrew Holmes, and Thomas L. Kash. Fear extinction requires infralimbic cortex projections to the basolateral amygdala. *Transl. Psychiatry*, 8(60):1–11, Mar 2018.

[9] Mohammed R. Milad, Christopher I. Wright, Scott P. Orr, Roger K. Pitman, Gregory J. Quirk, and Scott L. Rauch. Recall of Fear Extinction in Humans Activates the Ventromedial Prefrontal Cortex and Hippocampus in Concert. *Biol. Psychiatry*, 62(5):446–454, Sep 2007.

[10] Jinzhao Ji and Stephen Maren. Hippocampal Involvement in Contextual Modulation of Fear Extinction. *Hippocampus*, 17(9):749–758, 2007.

[11] Hiroyo Koseki, Machiko Matsumoto, Hiroko Togashi, Yoshihide Miura, Kazuaki Fukushima, and Mitsuhiro Yoshioka. Alteration of Synaptic Transmission in the hippocampal-mPFC Pathway During Extinction Trials of Context-Dependent Fear Memory in Juvenile Rat Stress Models. *Synapse*, 63(9):805–813, Sep 2009.

[12] D. Gowanlock R. Tervo, Bum-Yeol Hwang, Sarada Viswanathan, Thomas Gaj, Maria Lavzin, Kimberly D. Ritola, Sarah Lindo, Susan Michael, Elena Kuleshova, David Ojala, Cheng-Chiu Huang, Charles R. Gerfen, Jackie Schiller, Joshua T. Dudman, Adam W. Hantman, Loren L. Looger, David V. Schaffer, and Alla Y. Karpova. A Designer AAV Variant Permits Efficient Retrograde Access to Projection Neurons. *Neuron*, 92(2):372–382, Oct 2016.

[13] Peter Bankhead, Maurice B. Loughrey, José A. Fernández, Yvonne Dombrowski, Darragh G. McArt, Philip D. Dunne, Stephen McQuaid, Ronan T. Gray, Liam J. Murray, Helen G. Coleman, Jacqueline A. James, Manuel Salto-Tellez, and Peter W. Hamilton. QuPath: Open source software for digital pathology image analysis. *Sci. Rep.*, 7(16878):1–7, Dec 2017.

[14] Reference Atlas :: Allen Brain Atlas: Mouse Brain, Jul 2020. [Online; accessed 2. Jul. 2020].